Polymer 51 (2010) 2185–2190

Contents lists available at ScienceDirect

Polymer

journal homepage: www.elsevier.com/locate/polymer

Periodic nanocomposites: A simple path for the preferential self-assembly of nanoparticles in block-copolymers

Oz Gazit [a], Yachin Cohen [a], Rina Tannenbaum [a,b,*]

[a] Department of Chemical Engineering, Technion, Israel Institute of Technology, Haifa, Israel
[b] School of Materials Science and Engineering, Georgia Institute of Technology, Atlanta, GA 30332, USA

ARTICLE INFO

Article history:
Received 6 January 2010
Received in revised form
23 February 2010
Accepted 28 February 2010
Available online 24 March 2010

Keywords:
Block copolymers
Metallic nanoparticles
Periodic nanomaterials

ABSTRACT

The use of diblock copolymers as chemical templates for the self-assembly of patterned and periodic materials has been the focus of extensive research in recent years. In this current work we show how a "one-pot" solution synthesis, which is based solely on the differences in the chemical reactivity of the two blocks towards metallic moiety, can be extended to create 1-, 2- and 3-dimensional ordered arrays of nanoparticles, conforming to the microstructure of the diblock copolymer. Chromium oxide nanoparticles (Cr_2O_3) synthesized in a poly(styrene-*b*-methyl methacrylate) diblock copolymer solution form, after solvent evaporation and annealing, thin films consisting of a periodic composite material. We show that the preferential incorporation of the Cr_2O_3 nanoparticles into the diblock copolymer through the direct polymer block – metal interactions does not hinder the self-assembly mechanism or the thermodynamically-driven microstructure formation of the diblock copolymer. Results show that the preferential segregation that occurred as early as the mixing stage of the reaction components was maintained throughout the annealing stage and the formation of the bulk ordered composite material.

1. Introduction

The goal to manufacture devices with smaller dimensional features than those currently available through the traditional top-down approach, has proven to be very complex and highly expensive, particularly when structures in the nanoscale are contemplated [1,2]. Alternatively, the self-assembly of molecules and molecular fragments into a variety of multi-dimensional structures, may provide a relatively inexpensive route to produce nanometric scale materials via the non-traditional and surface-mediated bottom-up approach. Such a strategy is highly facilitated by the utilization of patterned substrates that can provide a suitable chemical or physical template for the directed assembly of various structures. Block copolymers (BCP) constitute a particularly suitable class of patterned chemical platforms for this emerging technology [1–3]. BCP consist of chemically different macromolecules or blocks, joined at their endpoints to form a single polymer chain. Since the free energy of mixing is unfavorable for intimate mixing of the two chemical species, the respective blocks tend to phase separate and form a variety of structures possessing one-, two-, or three-dimensional order [4–6]. Once the desired pattern is obtained, the ordered periodic structure can be functionalized to fit a desired application. For example, Kumar et al. used asymmetric polystyrene-b-poly(4-vinylpyridine) (PS-b-4PVP) to form spherical domains of PVP in PS matrix to create a two-dimensionally self-arranged protein nanoarrays [7].

The ability of BCP to self-assemble into spatially periodic structures makes them an excellent candidate in the building of photonic waveguides and photonic bandgap (PBG) materials [8–12]. The relationship between the block domain size, its refractive index and the resulting optical applicability of the BCP is given by the expression $\overline{d}_i \approx \lambda/4n_i$ (where n_i is the refractive index and d_i is the optical width, i.e. block domain size, of the *i*th domain). Hence, to obtain a BCP-based PBG material with a gap in the visible (~600 nm) or near-IR (~1000 nm) wavelength range, a large optical thickness of each layer, $n_i \cdot d_i$, is required. Since the refractive indices of polymers are relatively low (the average refractive index of polymeric materials is about 1.5) and the differences in the refractive indices between the polymer blocks are too small to be of significant usefulness (e.g. 1.59 for polystyrene and 1.51 for polyisoprene) [13], it becomes necessary to manipulate their morphology and composition in order to obtain the desired optical

* Corresponding author. School of Materials Science and Engineering, Georgia Institute of Technology, Atlanta, GA 30332, USA. Tel.: +1 404 385 1235; fax: +1 404 894 9140.
E-mail addresses: rinatan@mse.gatech.edu, rinatan@technion.ac.il (R. Tannenbaum).

0032-3861/$ – see front matter © 2010 Elsevier Ltd. All rights reserved.
doi:10.1016/j.polymer.2010.02.053

thickness required for such periodic materials. Several strategies have been developed to date in order to render these BCP assemblies technologically relevant: (a) To selectively swell the BCP domains by blending with low molecular weight homopolymers [13–18]. This method is limited in its applicability due to the very narrow range of BCP compositions that can sustain the same microstructure upon the addition of the homopolymer [15–18]. (b) To use block copolymers with very high molecular weights of both blocks and thus increase domain size [11]. However, these polymers would exhibit high viscosities, which in turn, may limit their processability. (c) Another alternative would be to increase the refractive index of one of the domains by adding nanoscale scatterers, without damaging the BCP spatial alignment. Upon transmission of light through such a nanocomposite, scattering intensity is substantially reduced when particle dimension is below 50–100 nm, and the optical characteristics of the composite material were shown to be strongly dependent on the particle size, shape, and the interactions between the polymer matrix and the metallic nanoclusters [19].

The manipulation of the refractive index rather than the domain size would enable the use of smaller domains obtained by lower molecular weight BCPs, which in general, provide better control over the processing characteristics of the BCP [20]. Hence, the selective introduction of nanoscale scatterers, such as metallic nanoparticles (NPs), into a particular BCP domain may provide an efficient strategy for the enhancement of the refractive index of that domain. The selective incorporation of metallic NPs into BCPs has been achieved to date through four main pathways: (a) The exposure of BCP films to metal vapors, resulting in the selective adsorption of metal atoms onto the more reactive block and the subsequent NP formation, as shown in the initial work of Morkved et al. [21], followed by the works of Horiuchi et al. [22], and Lopes and Jaeger [23]. (b) The impregnation of BCP films with a metal salt, followed by the reduction of the salt to form metallic NPs in the reactive block domains [24–27]. To date, this is the more widespread method and has been reported in several works of Möller et al. [27], Cohen et al. [24–26] and others. For example, Cohen et al. produced metal NPs by the loading of Pb into a di-BCP film and subsequently reacting it with H_2S to form PbS NPs with an average size of 4 nm [28]. The production of the PbS NPs was a multistep process, and the particle size was controlled by the number of similar Pb-loading cycles performed in the BCP film; (c) A third method for creating BCPs selectively filled with metal NPs of limited size and size distribution was developed by Thomas et al. [29]. This method consisted of the incorporation of CdSe nanocrystals into a styrene-isoprene-2-vinyl pyridine (SI-2VP) tri-BCP via their surface modification with surfactant molecules that were chemically similar and compatible with one of the blocks. Similarly, Bockstaller et al. incorporated gold NPs, coated with thiol-terminated PS, into a poly(styrene-b-ethylene/propylene) di-BCP [30], and Chiu et al. demonstrated control of the location of gold NPs in a poly(styrene-b-2-vinyl pyridine) di-BCP by coating the NPs surface with thiol-terminated PS and thiol-terminated PVP [31]. Despite the fact that these techniques provide the desired outcome, they involve the use metal clusters that have been pre-formed using the standard techniques for the formation of stabilized metal particles [9,13,14,32]. Subsequently the particles were introduced into the BCP solution and were directed to a particular block via the controlled interactions of the stabilizing molecules with the functional groups in a particular block. In this approach, the driving force for particle segregation is not the metal-polymer affinity, but the stabilizer–polymer interactions [33–35]. (d) The impregnation of pre-formed BCP films with organometallic precursors followed by the in-situ phase separation and assembly of the metallic nanoparticles in a preferred BCP microdomain. In this case, the BCPs are first allowed to self-assemble into their distinct microdomains, and subsequently exposed to the metallic moiety. If the polymers are below their T_g, the interfacial adhesion between polymer chains and the growing metallic fragments is severely hindered, and therefore, the limitation on metal nanoparticle size is due to nucleation and growth kinetics and not to a polymer "capping" effect [36].

We have developed a truly self-assembly approach, in which the nucleation and growth of the metal NPs and the phase separation of the BCPs occur concurrently and *in-situ*, in a homogenous solution comprised of both BCP and metal precursor. In such a system, the simultaneous coupling between the chemical reactivity of the metal clusters defined by their size and shape, and the difference in the reactivity of the blocks in the BCP, determine the polymer-metal NP interfacial interactions and the extent of phase separation process. The synthesis procedure that is designed to accommodate the manipulation of these variables consists of the decomposition of organometallic precursors under controlled conditions in the presence of a BCP solution [37–41]. The size of the NPs formed by this method is significantly influenced by the diffusion of small metallic fragments generated during the decomposition process through the medium and by the viscosity of the medium in which the diffusion takes place [40,41]. Under these conditions, the polymer in the solution acts as a barrier to the mobility of the growing NPs in the medium (by contributing to solution viscosity), and the reactive block in the polymer acts as the stabilizing molecule of the growing NPs. As a result, nucleation and growth of the NPs will be limited not only by reaction kinetics, but also by the direct interaction with the available reactive sites on the polymer. Hence, the difference in the reactivity of the two blocks toward the metal will be fully exhibited and can be fully exploited.

This work is an expansion and generalization of previous attempts to develop self-assembled periodic nanocomposites based on the segregation of NPs in a BCP template. By employing a "one-pot" synthesis, we were able to produce thin composite films with the metal oxide NPs directly embedded in a specific BCP domain, without the use of mediating or compatibilizing molecules such as surfactants and/or functionalized oligomers. Polystyrene-b-poly(methyl methacrylate) (PS-b-PMMA) is a good example of such a system due to the considerable difference between the weak dipole–dipole interactions of PS with the metal surface as compared to the much stronger interactions of PMMA with metallic surface sites via the formation of coordinative bonds [42,43]. Furthermore, we bring here the first example highlighting the preferential segregation of the metallic moiety in a metal-polymer composite via a self-assembly mechanism at the early stage of the introduction of the organometallic precursor into the BCP solution. This segregation is preserved despite the subsequent solvent elimination process and the formation of the composite films. Moreover, the ability of the BCP-metal composite system to self-assemble into the corresponding 1-,2- and 3- dimensional microstructures, as warranted by the thermodynamics of the pure BCP component under similar conditions, is not hindered by the presence of the segregated metallic phase.

2. Experimental

2.1. Decomposition reaction

A polymer, such as PS ($\overline{M}_n$ = 44,100 g/mol, PDI = 1.03, Polymer Source), PMMA ($\overline{M}_n$ = 46,500 g/mol, PDI = 1.04, Polymer Source) and PS-b-PMMA ($\overline{M}_n$ = 21,000-b-21,000 g/mol, PDI = 1.07, Polymer Source) was dissolved in cyclohexanone ($C_6H_{10}O$, 99.5%, d = 0.947 g/cm^3, b.p. = 155 °C, Fluka) to form a 2 wt.% polymer solution. A second solution composed of chromium hexacarbonyl

(99%, $Cr(CO)_6$, $d = 1.77$ g/cm^3, Aldrich) in cyclohexanone was also prepared. The solutions were left to stir dissolution. Reaction began with the mixing of both solutions in a flask under a constant nitrogen purge. Reaction flask was held at a constant temperature of 90 °C. During the reaction, aliquots were removed from the flask and quenched with an equal volume of cold solvent.

2.2. Particle and structure characterization

Particle size and morphology were examined by transmission electron microscopy (TEM) using FEI Tecnai G2T12 instruments. The operating voltage was 120 kV. Samples were prepared by placing a drop of the reaction on a carbon-coated copper grid (Ted Pella, Inc), with the excess solvent bloated off. Macromolecular structure was imaged using FEI Titan 80–300 keV FEG S/TEM in STEM mode with the High Angle Anular Dark Field detector (HAADF). Samples were prepared using a Reichert-Jung FC4E ultarmicrotom, equipped with a diamond knife, at room temperature, to obtain thin cross sections of the lamellar structure.

Small angle X-ray scattering measurements were performed using a small angle diffractometer (Bruker Nanostar, KFF CU 2 K-90) with CuK_α radiation, pinhole collimation (that yields a beam 100 μm in diameter) and a 10 × 10 cm^2, 2-dimensional position-sensitive wire detector positioned 65 cm behind the examined sample. Samples were placed in the camera with the structure positioned grazing angle relative to the source beam. Sample temperature was maintained at 25 °C. The patterns were recorded using acceleration voltage of 40 kV and acceleration current of 20 mA. The scattering patterns were circularly averaged and presented in terms of the intensity as function of the scattering vector q defined as, $q = (4\pi/\lambda)\sin\theta$, where 2θ is the scattering angle and $\lambda$is the wavelength of the CuK_α radiation (0.1542 nm).

3. Results and discussion

A typical "one-pot" synthesis is employed here for the formation of chromium oxide (Cr_2O_3) NPs selectively embedded in a PS-PMMA BCP matrix. This is achieved through the thermal decomposition of the chromium hexacarbonyl precursor, $Cr(CO)_6$ in the PS-PMMA block copolymer solution. The fundamental strategy that dictated the use of the PS-PMMA BCP was the fact that this system possesses chemically different segments, and on this basis, generates a reactivity gradient in the material that would preferentially direct the location of the NPs.

Previous studies have shown that the strong coordinative bond formed by the PMMA with the metallic fragments generated during the precursor decomposition reaction in solution, essentially dominates the formation mechanism of the NPs [36,42]. Therefore, it is expected that when the reaction is conducted in a BCP solution, the NPs will preferentially reside in the PMMA domain. Furthermore, it turns out that the preferential segregation of the metallic moiety in the PMMA domain originates at a much earlier stage, even prior to the formation of the NPs, i.e. as early as the precursor mixing stage. Due to the unfavorable interaction of PMMA with cyclohexanone compared to that of PS, it is expected that the BCP molecules would self-assemble into a micellar structure [44–47]. Despite this predicted behavior, we did not observe such structures in our pure BCP system, neither with SAXS measurements, nor with cryo-TEM imaging. However, upon the addition of the metal carbonyl precursor to the BCP solution, cryo-TEM images clearly show the formation of a dense PMMA domain structure (micelle-like), as shown in Fig. 1. Therefore, we can clearly state that the preferential segregation of the metal precursor into the PMMA domain occurs as early as the introduction of the metal precursor into the BCP solution. Hence, the synergetic contribution of the reaction components

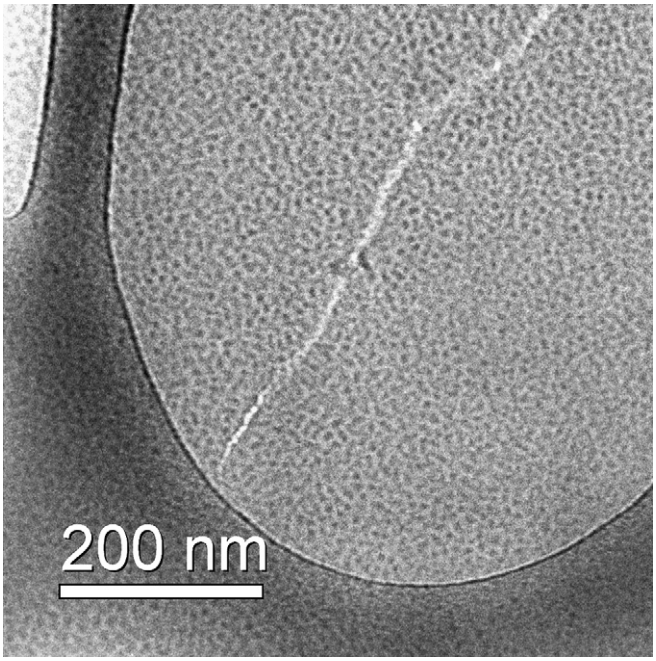

Fig. 1. Cryo-TEM image of a cyclohexanone solution of BCP with $Cr(CO)_6$ precursor. The solution was heated to 60 °C for a few minutes to obtain thermal equilibrium before vitrified in liquid N_2. The image shows BCP micelles having average dimensions of ~8 nm. The strong contrast arises from the presence of the organometallic precursor in the core of the micelles.

causes the formation of core-shell structures with the PMMA and metal precursor in the core and a PS corona. These observations, together with kinetic data pertaining to this system and similar systems, are further addressed in detail elsewhere [48].

Due to the strong interactions of PMMA with the NP surface sites, it is customary to think that particles inside a PS-b-PMMA matrix would preferentially reside in the PMMA domain [49]. However, to date, no direct evidence has been reported showing preferential sequestering of uncoated NPs in the PMMA domain. Fig. 2 shows a transmission electron microscopy (TEM) image of Cr_2O_3 NPs of uniform size ($D_{avg} = 2$ nm) and shape, which have been formed in the BCP solution and are therefore embedded in the corresponding BCP matrix before the solid polymer film sample was annealed. As is evident from Fig. 1, there is a homogenous distribution of the micelle-like structures that are loaded with the organometallic precursor in solution. Furthermore, the relatively low precursor concentration as compared to the BCP concentration (mass ratio of 1:19, respectively) and the mechanism by which the NPs are formed, result in the presence of only a small amount of NPs in each micelle. This observation can explain the reason for the similar homogenous distribution of NPs in the BCP matrix upon completion of the decomposition reaction, as seen in Fig. 2. This, in turn provides additional supports to the proposed conclusion that the precursor decomposition and the formation of the NPs occur in the confines of the PMMA domains [48].

When imaging unstained BCP samples, two important issues should be addressed: (a) Because the grainy pattern of the BCP is similar in size and shape to the NPs, it is difficult to differentiate between the two moieties, which makes it difficult to prove the existence of preferential segregation of the NPs in one of the blocks; (b) Differences in contrast under TEM microscope can also be the result of radiation damage caused by the electron beam. The encounter of the electron beam with the sample may cause scission of the PMMA side chains, but at the same time, have little effect on the PS, which is much more stable under these conditions. This can

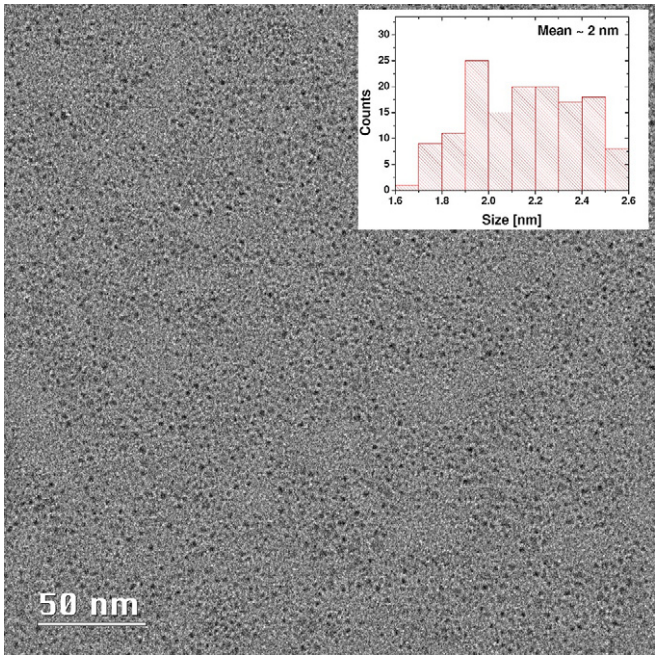

Fig. 2. TEM image of Cr_2O_3 NPs dispersed in BCP before annealing. The insert shows size distribution graph where at least 150 NPs were measured. Average size was calculated to be 2.2 ± 0.2 nm.

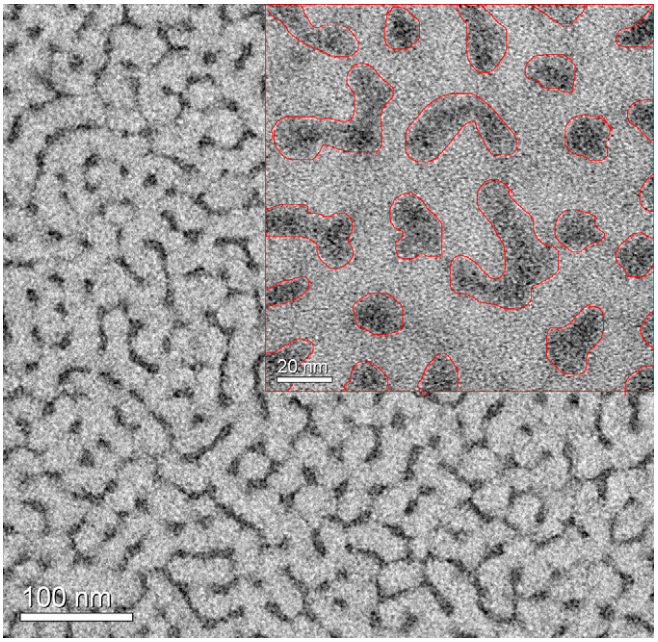

Fig. 3. TEM image of Cr_2O_3 NPs embedded in an asymmetric BCP after 2 days of annealing. Measurements of the size of PMMA cylindrical domains to the PS matrix gives a 1:3 ratio, which is in agreement with the molar ratio of the BCP blocks.

be responsible for the mass differences seen in the TEM image [50]. To overcome difficulties and/or artifacts in image analysis and erroneous image interpretations due to resolution, contrast and radiation damage, a low dose mode was used during imaging on the microscope. Furthermore, the synthesis of the NPs was performed using asymmetric BCP, such that the molar ratio of the two blocks would generate the cylindrical microstructure in the melt (~26 wt.% PMMA block, out of a total molecular weight of 33,500 g/mol), as shown in Fig. 3. Since the thermodynamics-driven, ordered, periodic domain structure of BCPs is formed in the melt, the reaction solution was deposited drop wise on a copper grid and subsequently annealed at 165 °C for 2 days under vacuum. A random arrangement of cylindrical morphology, in accordance with the molecular weight ratios of the two blocks in the BCP, is seen with hexagonal order appearing only in part of the image. In this case the PMMA domains are smaller compared to those of the PS, forcing the NPs to arrange more densely and therefore, the contrast that they generate compared to their polymeric surroundings is much better evidenced. Based on this image, it is easy to realize that the NPs are concentrated in the smaller BCP domain, i.e., that of the PMMA block. Using the respective asymmetric BCP molecular weights for PS (24,500 g/mol) and PMMA (9000 g/mol) blocks and by assuming bulk homopolymer densities (1.06 g/cm^3 and 1.188 g/cm^3 respectively [51]), we are able to evaluate the partial volume occupied by each of the polymer blocks in the BCP thin film. Our calculations show that the volumetric ratio between the domains is 3:1 PS to PMMA. Because of the high field depth in TEM imaging and the thin sample, all structures are in focus simultaneously regardless of sample thickness. Therefore, by integrating the number of pixels in the contour surrounding the dark areas (see insert in Fig. 3) with respect to the rest of the image area, we can evaluate the volume ratio between the PS domain to the PMMA domain to be 5:2, respectively. This rough analysis clearly indicates the occurrence of some swelling of the PMMA domain as a result of the preferential segregation of the NPs into that domain. Further examination of the volumetric contribution of the Cr_2O_3 NPs (using an average Cr_2O_3 particle diameter of 2 nm, a bulk density of 5.21 g/cm^3 and assuming spherical morphology) gives a total NPs volume of roughly 10^{-3} cm^3. This indicates that the presence of the NPs in the concentration we used has a minor effect on the volume of the PMMA domain. However, the apparent difference in volume ratios between the PMMA and PS domains, with and without the NPs, is attributed to the effective volume contribution caused by the adsorption of the polymeric chains, predominantly PMMA, onto the surface of the NPs [52,53].

Since the partitioning of the NPs is dependent on the chemical make-up of the BCP, in this case PS and PMMA, it should be possible to expand this approach to obtain preferential segregation in all other dimensional morphologies available by the self-assembly of a BCP containing these same blocks.

Fig. 4 shows a scanning TEM (STEM) image of a symmetric BCP/NPs composite (i.e., $f_{PS}/f_{PMMA} \approx 1$,) after annealing. The use of STEM is convenient due to the fact that the large atomic number of the chromium results in a considerable contrast difference compared to the polymeric domain [54]. The image demonstrates the existence of an extensive large scale lamellar orientation of the BCP blocks,

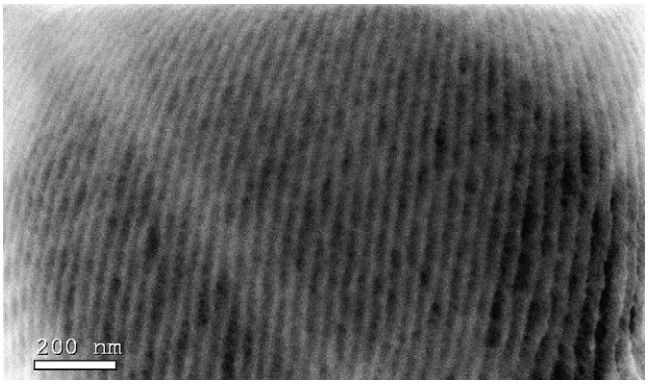

Fig. 4. Cross section STEM image of aligned symmetric BCP/NPs composite film. The measured periodicity is ~27 nm.

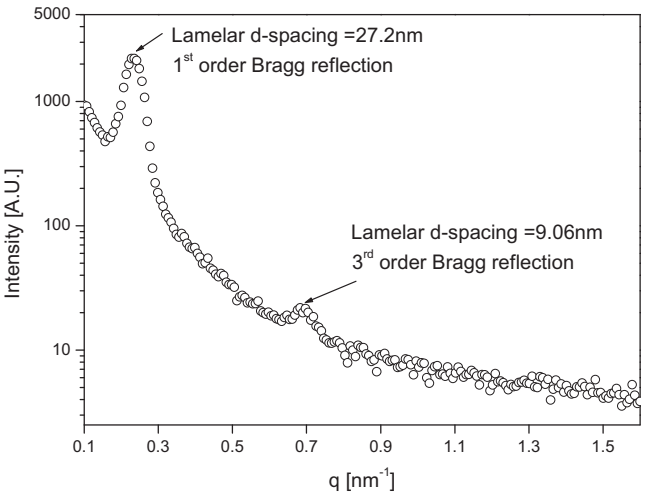

Fig. 5. SAXS data obtained from a block copolymer film containing chromium oxide NPs. The direction of the incident beam is parallel to the orientation of the lamellae. Calculating the relative dimension between the two peaks equals 3, corresponding to first and third order Bragg reflection.

with the NPs preferentially concentrated in only one of the periodic domains (i.e. PMMA).

To examine the possibility of using this complex material for photonic bandgap applications, the structure must be organized and the domains aligned over several length scales to extend into the macro-scale. Fig. 5 shows small angle x-ray scattering (SAXS) measurements, performed at grazing incidence geometry (GI), parallel to the substrate. The semi log plot shows both first and third order Bragg reflection related to a lamellar periodic dimension of ~27.2 nm. The measured d-spacing is in good agreement with the periodic dimension of ~27 nm extracted from the STEM images. The periodic dimension is also in agrement with an empiric equation given by Coulon et al. for PS-b-PMMA in the weak segregation limit, $d = 13.5N^{1/2}$, where N is the total number of monomer segments in the copolymer [55]. STEM and SAXS measurements show that the thermodynamics-driven self-assembly of the BCP/NPs composite was not hindered due to the reactive embedding of the chromium oxide NPs in the preferential domain, i.e. the PMMA domain.

4. Conclusions

In summary, we have shown that it is possible to create a periodic self-assembled BCP-metallic NPs composite material using a self-assembly approach and without the need of intermediate molecules. Utilizing the difference in the chemical make-up between BCP segments, metallic NPs are synthesized such that they would preferentially reside in one specific domain. Because the composite material is formed through a self-assembly process, the final structure is thermodynamically very stable. Moreover, since the structure is controlled by the type of BCP used, it would be very easy to manipulate the spatial arrangement of the nano-composite into much more complicated structures, such as tri-BCP, star-BCP etc. Although this work focuses on the preferential segregation of Cr_2O_3 NPs in di-BCPs, it is easily extendable to other metal-oxides that may be synthesized using metal carbonyl precursors, as evidenced from other publications by our group (i.e. see reference [48]).

This paper serves as a proof of concept for a simple one-pot method to create a periodic array of metallic scatterers. However, the periodic dimensions shown here are relatively small and the challenge to create this ordered composite material with larger periodicities is a subject for further research, if a PBG material is to be made.

Acknowledgments

This research was supported by the Israel Science Foundation, Grant Nr. 650/06, by the European Union Marie Curie International Reintegration Grant (IRG), Nr. 036577, and by The National Science Foundation, Award ID ECS-0535382. The authors are indebted to Ms. Yehudit Schmidt from the Department of Chemical Engineering at the Technion for her expertise and assistance with the TEM imaging.

References

[1] Krishnamoorthy S, Hinderling C, Heinzelmann H. Materials Today 2006;9:40.
[2] Li M, Ober CK. Materials Today 2006;9:30.
[3] Cheng JY, Ross CA, Smith HI, Thomas EL. Advanced Materials 2006;18:2505.
[4] Bates FS, Fredrickson GH. Annual Review of Physical Chemistry 1990;41:525.
[5] Hiemenz PC. Polymer chemistry-the basic concepts. Marcel Dekker, Inc.; 1984.
[6] Ohta T, Ito A. Physics Review E 1995;52:5250.
[7] Kumar N, Parajuli O, Hahm JI. Journal of Physical Chemistry B 2007;111:4581.
[8] Chen JT, Thomas EL, Zimba CG, Rabolt JF. Macromolecules 1995;28:5811.
[9] Fink Y, Winn JN, Fan S, Chen C, Michel J, Joannopoulos JD, et al. Science 1998;282:1679.
[10] Lin Y, Boker A, He J, Sill K, Xiang H, Abetz C, et al. Nature 2005;434:55.
[11] Yoon J, Lee W, Thomas EL. MRS Bulletin 2005:721.
[12] Bockstaller MR, Mickiewicz RA, Thomas EL. Advanced Materials 2005;17:1331.
[13] Fink Y, Urbas AM, Bawendi MG, Joannopoulos JD, Thomas EL. Journal of Lightwave Technology 1999;17:1963.
[14] Urbas AM, Fink Y, Thomas EL. Macromolecules 1999;32:4748.
[15] Winey KI, Gobran DA, Xu ZD, Fetters LJ, Thomas EL. Macromolecules 1994;27:2392.
[16] Winey KI, Thomas EL, Fetters LJ. Macromolecules 1991;24:6182.
[17] Winey KI, Thomas EL, Fetters LJ. Macromolecules 1992;25:422.
[18] Winey KI, Thomas EL, Fetters LJ. Macromolecules 1992;25:2645.
[19] Pinna N, Maillard M, Courty A, Russier V, Pileni MP. Physics Review B 2002;66:045415.
[20] Gosa KL, Serban S, Christopoulou V, Papanagopoulos D, Dondos A. Polymer-Plastics Technology and Engineering 2000;39:95.
[21] Morkved TL, Wiltzius P, Jaeger HM, Grier DG, Witten TA. Applied Physics Letters 1994;64(4):422.
[22] Horiuchi S, Sarwar MI, Nakao Y. Advanced Materials 2000;12(20):1507.
[23] Lopes WA, Jaeger HJ. Nature 2001;414:735–8.
[24] Clay RT, Cohen RE. Supramolecular Science 1995;2:183.
[25] Kane RS, Cohen RE, Sibley R. Chemistry of Materials 1996;8:1919.
[26] Ciebien JF, Cohen RE, Duran A. Supramolecular Science 1998;5:31.
[27] Spatz JP, Mössmer S, Hartmann C, Möller M, Herzog T, Krieger M, et al. Langmuir 2000;16:407.
[28] Clay RT, Cohen RE. Chemistry of Materials 1996;8:1919.
[29] Fink Y, Urbas AM, Bawendi MG, Joannopolous JD, Thomas EL. Journal of Lightwave Technology 1999;17(11):1963.
[30] Bockstaller M, Kolb R, Thomas EL. Advanced Materials 2001;13:1783.
[31] Chiu JJ, Kim BJ, Kramer EJ, Pine DJ. Journal of the American Chemical Society 2005;127:5036.
[32] Joly S, Kane R, Radzilowski L, Wang T, Wu A, Cohen RE, et al. Langmuir 2000;16:1354.
[33] Hashimoto T, Harada M, Sakamoto N. Macromolecules 1999;32:6867.
[34] Zhou C, Deshpande MR, Reed MA, Jones L, Tour JM. Applied Physics Letters 1997;71:611.
[35] Jana NR, Gearheart L, Murphy CJ. Advanced Materials 2001;13:1389.
[36] Gazit O, Dan N, Tannenbaum R. Macromolecules 2008;41:2164.
[37] Tannenbaum R, Goldberg EP, Flenniken CL. Metal-containing polymeric systems. New York: Plenum Press; 1985.
[38] Griffiths CH, Ohoro MP, Smith TW. Journal of Applied Physics 1979;50:7108.
[39] Tannenbaum R, Flenniken CL, Goldberg EP. Journal of Polymer Science Part B – Polymer Physics 1990;28:2421.
[40] Klabunde KJ, Tanaka Y. Journal of Molecular Catalysis 1983;21:57.
[41] Kanai H, Tan BJ, Klabunde KJ. Langmuir 1986;2:760.
[42] Tadd EH, Bradley J, Tannenbaum R. Langmuir 2002;18:2378.
[43] Dan N, Zubris M, Tannenbaum R. Macromolecules 2005;38(22):9243.
[44] Fukumine Y, Inomata K, Takano A, Nose T. Polymer 2000;41:5367.
[45] Hanley KJ, Lodge TP, Huang CI. Macromolecules 2000;33(16):5918.
[46] Li Z, Zhao W, Liu Y, Rafailovich MH, Sokolov J, Khougaz K, et al. Journal of the American Chemical Society 1996;118:10892.
[47] Mortensen K, Brown W, Almdal K, Alami E, Jada A. Langmuir 1997;13:3635.

[48] Gazit O, Khalfin R, Cohen Y, Tannenbaum R. Journal of Physical Chemistry C 2008;113(2):576.
[49] Deshmukh RD, Buxton GA, Clarke N, Composto RJ. Macromolecules 2007;40:6316.
[50] Thomas EL, Talmon Y. Polymer 1978;19:225.
[51] Sperling LH. Introduction to physical polymer science. 3rd ed. New York: John Wiley & Sons Inc; 2001.
[52] Hershkovitz E, Tannenbaum A, Tannenbaum R. Journal of Physical Chemistry B 2008;112(17):5317–26.
[53] Hershkovitz E, Tannenbaum A, Tannenbaum R. Macromolecules 2008;41 (9):3190–8.
[54] Lyman CE. Encyclopedia of materials characterization. Butterworth-Heinemann; 1992.
[55] Coulon G, Russell TP, Deline VR, Green PF. Macromolecules 1989;22(6):2581.